

# Multiplexing oscillatory biochemical signals

Wiet de Ronde<sup>1</sup> and Pieter Rein ten Wolde<sup>1</sup>

<sup>1</sup>FOM Institute AMOLF, Science Park 104, 1098 XG Amsterdam, The Netherlands

In recent years it is increasingly being recognized that biochemical signals are not necessarily constant in time and that the temporal dynamics of a signal can be the information carrier. Moreover, it is now well established that components are often shared between signaling pathways. Here we show by mathematical modeling that living cells can multiplex a constant and an oscillatory signal: they can transmit these two signals through the same signaling pathway simultaneously, and yet respond to them specifically and reliably. We find that information transmission is reduced not only by noise arising from the intrinsic stochasticity of biochemical reactions, but also by crosstalk between the different channels. Yet, under biologically relevant conditions more than 2 bits of information can be transmitted per channel, even when the two signals are transmitted simultaneously. These observations suggest that oscillatory signals are ideal for multiplexing signals.

## I. INTRODUCTION

Cells live in a highly dynamic environment, which means that they continually have to respond to a large number of different signals. One possible strategy for signal transmission would be to use distinct signal transduction pathways for the transmission of the respective signals. However, it is now clear that components are often shared between different pathways. Prominent examples are the Mitogen-Activated Protein Kinase (MAPK) signaling pathways in yeast, which share multiple components [1, 2]. In fact, cells can even transmit different signals through one and the same pathway, and yet respond specifically and reliably to each of them. Arguably the best-known example is the rat PC-12 system, in which the epidermal growth factor (EGF) and neuronal growth factor (NGF) stimuli are transmitted through the same MAPK pathway, yet give rise to different cell fates, respectively differentiation and proliferation [3, 4]. Another example is the p53 system, in which the signals representing double-stranded and single-stranded breaks in the DNA are transmitted via the same pathway [5]. These observations suggest that cells can *multiplex* biochemical signals [6], *i.e.* transmit multiple signals through one and the same signaling pathway, just as many telephone calls can be transmitted simultaneously via a shared medium, a copper wire or the ether.

One of the key challenges in transmitting multiple signals via pathways that share components is to avoid unwanted crosstalk between the different signals. In recent years, several mechanisms for generating signaling specificity have been proposed. One strategy is spatial insulation, in which the shared components are recruited into distinct macromolecular complexes on scaffold proteins [1, 7]. This mechanism effectively creates independent communication channels, one for each signal to be transmitted. Another mechanism is kinetic insulation, in which the common pathway is used at different times, and a temporal separation between the respective signals is thus established [8]. Another solution is cross-pathway inhibition, in which one signal dominates the

response [9–13]. In the latter two schemes, kinetic insulation and cross-pathway inhibition, the signals are effectively transmitted via one signaling pathway, though in these schemes multiple messages cannot be transmitted simultaneously.

We have recently demonstrated that cells can truly multiplex signals: they can transmit at least two signals simultaneously through a common pathway, and yet respond specifically and reliably to each of them [6]. In the multiplexing scheme that we proposed, the input signals are encoded in the concentration levels of the signaling proteins. The underlying principle is, however, much more generic, since essentially any coding scheme can be used to multiplex signals. This observation is important, because it is becoming increasingly clear that cells employ a wide range of coding strategies for transducing signals. One is to encode the signals in the duration of the signal. This is the scheme used by the NGF-EGF system: while EGF stimulation yields a transient response of ERK, NGF leads to a sustained response of ERK [3, 4]. Another strategy is to encode the message in the frequency or amplitude of oscillatory signals. Indeed, a large number of systems have now been identified that employ oscillatory signals to transduce information. Arguably the best-known example is calcium oscillations [14], but other examples are the p53 [5], NFAT [15, 16], nuclear ERK oscillations [17] and NF- $\kappa$ B system [15, 18–20]. In fact, cells use oscillatory signals not only to transmit information intracellularly, but also from one cell to the next—insulin [21] and Gonadotropin Release Hormone (GnRH) [22] are prominent examples of extracellular signals that oscillate in time. More examples of systems that encode stimuli in the temporal dynamics of the signal are provided in the recent review article by Behar and Hoffmann [23].

In this manuscript we demonstrate that oscillatory signals can be used to multiplex biochemical signals. We present a multiplexing system, which is based on well-known network motifs, such as the Goldbeter-Koshland push-pull network [24] and the incoherent feedforward motif [25]. For the constant signal the information is encoded in the concentration, while for the oscillatory signal

the message is encoded in the amplitude or the frequency of the oscillations. These input signals are then multiplexed in the dynamics of a common signaling pathway, which are finally decoded by downstream networks.

Our results highlight that information transmission is a mapping problem. For optimal information transmission, each input signal needs to be mapped onto a unique output signal, allowing the cell to infer from the output what the input was. It is now well established that noise, arising from the inherent stochasticity of biochemical reactions, can reduce information transmission [6, 20, 26–31], because a given output signal may correspond to different input signals. Additionally, here we show that crosstalk between the two different signals can also compromise information transmission: a given state of a given input signal can map onto different states of its corresponding output signal, because the input-output mapping for that channel depends on the state of the signal that is transmitted through the other channel. This crosstalk presents a fundamental bound on the amount of information that can be transmitted, because it limits information transmission even in the deterministic, mean-field limit. We also show, however, that under biologically relevant conditions more than 2 bits of information can be transmitted per channel. We end by comparing our results with observations on experimental systems, in which oscillatory and constant signals are transmitted through a common pathway.

## II. RESULTS

### A. The model

Fig. 1 shows a cartoon of the setup. We consider two input species  $S_1$  and  $S_2$ , with two corresponding output species,  $X_1$  and  $X_2$ , respectively. The concentration  $S_1(t)$  of input  $S_1$  oscillates in time, while the concentration of  $S_2$  is constant in time. An input signal can represent different messages; that is, the input can be in different states. For  $S_1$  the different states could either be encoded in the amplitude or in the period of the oscillations. Here, unless stated otherwise, we will focus on the former and comment on the latter in the Discussion. The different states of  $S_2$  correspond to different copy-number or, since we are working at constant volume, concentration levels  $S_2$ . The signals  $S_1$  and  $S_2$  drive oscillations in the concentration  $V(t)$  of an intermediate component  $V$ , with a mean that is determined by  $S_2$  and an amplitude that is determined by  $S_1$  (see *SI*). The states of  $S_1$  are thus encoded in the amplitude of  $V(t)$  while the states of  $S_2$  are encoded in the mean level of  $V$ . The output  $X_2$  reads out the mean of  $V(t)$  and hence the state of its input  $S_2$  by simply time-integrating the oscillations of  $V(t)$ . The output  $X_1$  reads out the amplitude of the oscillations in  $V(t)$  and hence the state of  $S_1$  via an adaptive network, indicated by the dashed circle. We now describe the coding and decoding steps in more detail.

### 1. Encoding

In the encoding step of the motif, the two signals  $S_1$ ,  $S_2$  are combined into the shared pathway. The signals are modeled as a sinusoidal function

$$S(t) = \mu \left( 1 + A \sin \left( 2\pi \frac{t}{T} \right) \right). \quad (1)$$

$\mu$  is the signal mean,  $A$  is the signal amplitude and  $T$  is the period of the signal oscillation. We assume that the signals are deterministic and discuss the effects of noise later. As discussed above,  $S_1$  is an oscillatory signal, with kinetic parameters  $A_1, T_1$  and constant  $\mu_1$ .  $S_2$  is constant,  $A_2 = 0$ , and the concentration level  $\mu_2$  carries the information (i.e. sets the state) in the signal. In recent years it has been shown that biochemical systems can tune separately the amplitude and frequency of an oscillatory signal [32, 33].

The simplest shared pathway is a single component,  $V$ , which could be a receptor on the cell or nuclear membrane, but could also be an intracellular enzyme or a gene regulatory protein. We imagine that each signal is a kinase for  $V$ , which can switch between an active (e.g. phosphorylated) state ( $V^P$ ) and an inactive (e.g. unphosphorylated) state, such that

$$\frac{dV^P}{dt} = \frac{k_V [\sum_i S_i(t)] (V_T - V^P)}{K_V + (V_T - V^P)} - m_V E_T \frac{V^P}{M_V + V^P}, \quad (2)$$

where we sum over the two signals  $S_1(t)$  and  $S_2(t) = \mu_2$ . The dephosphorylation is mediated by a phosphatase, that has a constant copy number  $E_T$ . In Eq. 2 we assume Michaelis-Menten dynamics for  $V$  (see *SI* for more details).

The Michaelis-Menten kinetics of the activation of  $V$  could distort the oscillatory signal of  $S_1$ . They could reduce the amplitude of the oscillations or transform the sinusoidal signal into a signal that effectively switches between two values. Such transformations potentially hamper information transmission. We therefore require that the component  $V$  accurately tracks the dynamics of the input signals. It is well known that a linear transfer function between  $S$  and  $V$  does not lead to a deformation of the dynamic behavior, but only to a rescaling of the absolute levels (see *SI*). A linear transfer function can be realized if the kinase acts in the saturated regime, while the phosphatase is not saturated ( $K_V \ll (V_T - V^P(t))$ ,  $M_V \gg V^P(t)$ ), leading to

$$\frac{dV^P}{dt} = k_V \left( \sum_i S_i(t) \right) - m'_V V^P. \quad (3)$$

with  $m'_V = m_V E_T / M_V$ .

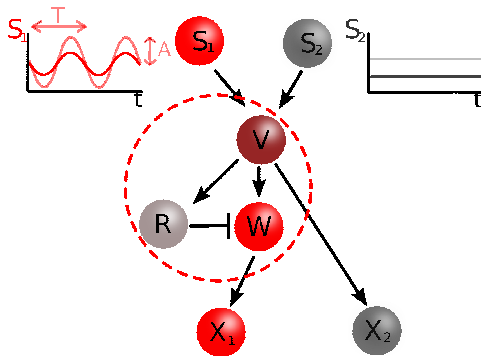


FIG. 1. Schematic drawing of the multiplexing system. Two signals are multiplexed. Signal  $S_1$  oscillates in time while signal  $S_2$  is constant. The message of  $S_1$  could either be encoded in the amplitude or the frequency of the oscillations, but in this manuscript we focus on the former. The message of  $S_2$  is encoded in the concentration. The output or response of  $S_1$  is  $X_1$  while the response of  $S_2$  is  $X_2$ . Encircled is the adaptive motif, used to readout the amplitude of the oscillations of  $S_1$ .

## 2. Decoding $V^P$ to $X_1, X_2$

The second part of the multiplexer is the decoding of the information in  $V^P$  into a functional output (see Fig. 1). The signals that are encoded in  $V^P$  have to be decoded into two output signals, the responses  $X_1$  and  $X_2$ . We imagine that the cell should be able to infer from an instantaneous measurement of the output response the state of the corresponding input signal. Therefore, we take the outputs of the multiplexing motif to be the concentration levels  $X_1$  and  $X_2$  of the output species  $X_1$  and  $X_2$ , respectively. Here  $X_1$  is the response of  $S_1$ , while  $X_2$  is the response of  $S_2$ .

The response  $X_2$  should be sensitive to the concentration of  $S_2$ , but be blind to any characteristics of  $S_1$ . In our simple model there is only one time-dependent signal, namely  $S_1$ ;  $S_2$  is constant in time. Since  $V^P$  has a linear transfer function of the signals (Eq. 3), the average level of  $V^P$ ,  $\langle V^P \rangle$ , is independent of both the amplitude  $A_1$  and the period  $T_1$  of the oscillations in  $S_1$ .  $\langle V^P \rangle$  does depend on the mean concentration level of the two signals, and since  $S_1$  has a constant mean, changes in  $\langle V^P \rangle$  reflect only a change in the mean of  $S_2$ ,  $\mu_2$ . As a result, a simple linear time integration motif can be used as the final read out for  $S_2$ . We therefore model  $X_2$  as

$$\frac{dX_2}{dt} = k_{X_2} V^P(t) - m_{X_2} X_2(t). \quad (4)$$

Since Eq. 4 is linear,  $\langle X_2 \rangle$  is a function of  $\langle V^P \rangle$  only. Moreover, if the response time of  $X_2$ ,  $\tau_{X_2} (= m_{X_2}^{-1})$ , is much longer than the oscillation period  $T_1$  of  $S_1$ , the effect of the oscillations on the instantaneous concentration  $X_2$  is integrated out. This is important to reduce the variability in  $\langle X_2 \rangle$  due to dynamics in the system [34].

For  $X_1$  a simple time-integration scheme does not work. The information that has to be mapped onto the output concentration  $X_1$  is the amplitude of  $S_1$ , which is propagated to  $V^P$ . The output  $X_1$  should therefore depend on the amplitude of the oscillations of  $V^P$ , but not on

its mean  $\langle V^P \rangle$ , since the mean represents the information in  $S_2$ . These requirements mean that the frequency-dependent gain of the network from  $V$  to  $X_1$  should have a band-pass structure. The frequency-dependent gain shows how the amplification of the input signal depends on the frequency of the signal [35] (Fig. 2). Due to the finite lifetime of the molecules, the frequency-dependent gain of any biochemical network inevitably reaches zero at high frequencies. Here we require that at the other end of the frequency spectrum, in the zero-frequency limit, the gain should also be small: Changes in the constant level of  $V^P$ , which result from changes in  $S_2$ , should not be amplified because  $X_1$  should not respond to changes in  $S_2$ . Indeed, only at intermediate frequencies should the gain be large: Changes in the amplitude of the oscillations of  $V^P$  at the frequency of the input  $S_1$  must be strongly amplified, because these changes correspond to changes in  $S_1$  to which  $X_1$  must respond. The network between  $V$  and  $X_1$  should thus have a frequency-transmission band that matches the frequency of  $S_1$ . The output  $X_1$  will then strongly respond to  $S_1$  but not to  $S_2$ .

A common biochemical motif with a frequency band-pass filter is an adaptive motif [36]. An adaptive system does not respond to very slowly varying signals, essentially because it then already adapts to the changing signal before a response is generated. Indeed, the key feature of an adaptive system is that the steady-state output is independent of the magnitude of a constant input, meaning that

$$\langle W \rangle = f(\{\text{all parameters}\} \notin \langle V^P \rangle). \quad (5)$$

This appears to be precisely what is required, because it means that when  $S_1$  is absent and  $S_2$  is changed, the output  $X_1$  remains constant, as it should — only  $X_2$  should change when  $S_2$ , a signal constant in time, is changed. On the other hand, while the steady-state output of an adaptive network is insensitive to variations in constant inputs, it is sensitive to dynamical inputs. This obser-

vation is well known; it is, e.g., the basis for the chemotactic behavior of *E. coli*, where the system responds to a change in the input concentration, and the strength of the response depends on the magnitude of the change in input concentration. This is another characteristic that is required, because it allows the magnitude of the response  $X_1$  to depend on the amplitude  $A_1$  of the oscillations in  $S_1$ , thus enabling a mapping from  $A_1$  to  $X_1$ . The important question that remains is whether the magnitude of the response solely depends on the change in the input concentration, which reflects  $S_1$ , or whether it also depends on the absolute value of the input concentration, which reflects  $S_2$ . In the following, we will show that it may depend on both, which would introduce crosstalk between the two signals.

Two common ways to construct an adaptive motif are known [37], the negative feedback motif and the incoherent feed-forward motif. In this multiplexing system we use the latter. In the incoherent feed-forward motif the input signal, in our case  $V^P$ , stimulates two downstream components R, W, see Fig. 1. One of the downstream components, R, is also a signal for the other downstream component, W. Importantly, the regulatory effect of the direct pathway ( $V^P \rightarrow W$ ) is opposite to the effect of the indirect pathway ( $V^P \rightarrow R \rightarrow W$ ). As a result, if  $V^P$  activates W, this activation is counteracted by the regulation of W through R. We thus obtain

$$\frac{dR}{dt} = k_R V^P - m_R R, \quad (6)$$

$$\frac{dW}{dt} = k_W \frac{V^P (W_T - W^P)}{K_W + (W_T - W^P)} - m_W \frac{RW^P}{M_W + W^P}. \quad (7)$$

This motif is adaptive, which can be shown by setting the time-derivatives in Eq. 6 and Eq. 7 to zero and solving for the steady state  $\langle W^P \rangle$ . This yields

$$0 = \frac{(k_W (W_T - \langle W^P \rangle)) (m_R (\langle W^P \rangle + M_W))}{(K_W + (W_T - \langle W^P \rangle)) (m_W k_R \langle W^P \rangle)}. \quad (8)$$

Although the full expression for  $\langle W^P \rangle$  is unwieldy to present, Eq. 8 shows that it does not depend on the magnitude of a constant input  $\langle V^P \rangle$ , which means that the network is indeed adaptive.

For a correct separation of the signals, the response  $W$  should be insensitive to the average level of  $V^P$ ,  $\langle V^P \rangle$ , since  $\langle V^P \rangle$  carries information on  $S_2$ , and not  $S_1$ . Indeed, a dependence of W on  $\langle V^P \rangle$  and hence on  $S_2$  necessarily leads to unwanted crosstalk between the two information channels. While the adaptive property of the network ensures that  $W^P$  is insensitive to the mean of  $V^P$  for a constant input (see Eq. 8), this is not necessarily the case for a dynamic  $V^P(t)$ . Since Eq. 7 is non-linear, the response  $W$  is dependent on the precise functional form of  $V^P$ , and, more importantly, will depend on  $\langle V^P \rangle$ . Crosstalk may thus arise, which will be studied in more detail below.

The full expression of the frequency-dependent gain  $g^2(\omega)$  is too unwieldy to present here, but in simplified

form we have

$$g_{W^P}^2(\omega) \propto \frac{\alpha \omega^2}{\beta (\omega^2 + \tau_R^{-2}) (\omega^2 + \tau_W^{-2}) (\omega^2 + \tau_V^{-2})}, \quad (9)$$

where  $\alpha$  and  $\beta$  are proportionality constants and  $\tau_i$  are the response times of component  $i$ . For slowly varying signals ( $\omega \rightarrow 0$ ), the amplitude of the response is negligible due to the  $\omega^2$ -term in the numerator of Eq. 9, reflecting the adaptive nature of the network. Second, for  $\omega \ll \min[\tau_V^{-1}, \tau_R^{-1}, \tau_W^{-1}]$ , the power scales with  $\omega^2$ . For very large  $\omega$  the power scales with  $\omega^{-4}$ . In the intermediate regime for  $\omega$ , the scaling depends on the precise response times. The response times are the diagonal Jacobian elements for the linearized system (Eqs. 2,6,7),

$$\tau_V = \left[ \frac{m_V E_T M_V}{(M_V + \langle V^P \rangle)^2} + \frac{k_V K_V \mu}{(V_T - \langle V^P \rangle + K_V)^2} \right]^{-1}, \quad (10)$$

$$\tau_R = m_R^{-1}, \quad (11)$$

$$\tau_W = \left[ \frac{m_W M_W \langle R \rangle}{(M_W + \langle W^P \rangle)^2} + \frac{k_W K_W \langle V^P \rangle}{(W_T - \langle W^P \rangle + K_W)^2} \right]^{-1}. \quad (12)$$

Eq. 11 gives the response time for a protein with a simple birth-death reaction. The mathematical form of the response times,  $\tau_V$  and  $\tau_W$ , Eq. 10 and Eq. 12, resembles that of a switching process with a forward and a backward step; their values depend on the signal parameters. When the dynamics of  $V^P$  operate in the linear regime (see Eq. 3),  $\tau_V$  simplifies to  $\tau_V \approx -(m_V E_T / (M_V))^{-1}$ , which is just the linear decay rate of  $V^P$ . Importantly, while  $\langle W^P \rangle$  is independent of the state  $\mu_2$  of  $S_2$ , the response time  $\tau_W$  and hence the gain  $g^2(\omega)$  do depend on  $\langle V^P \rangle$  and thereby on  $S_2$ . This means that the response of  $X_1$  to  $S_1$  will depend on  $S_2$ , generating crosstalk.

The gain (Eq. 9) is shown in Fig. 2a,b for two different parameter sets. The bandpass structure, with corresponding resonance frequency (the peak in the gain) is observed. Further, with circles, the response times  $\tau_V$  (black open),  $\tau_R$  (black solid) and  $\tau_W$  (gray open) are shown, which determine the position of the peak in the gain; the peak occurs at a frequency in between the two largest response times. In Fig. 2a we observe the influence of increasing  $k_R, m_R$ , which are taken to be equal. For very slow changes in  $R$ , corresponding to  $k_R, m_R$  being small, the network has a very large gain. Increasing the response time of  $R$ , decreases the amplitude at the resonance frequency considerably. Faster tracking of  $V^P$  by  $R$  makes the adaptation of the biochemical circuit very fast and as a result,  $W^P$  does not respond at all to changes in  $V^P$ . In Fig. 2b we observe the influence of changing the state  $\mu_2$  of  $S_2$ . The gain decreases for larger  $\mu_2$ , and the response time  $\tau_W$  increases. This may lead to crosstalk, since the mapping of  $A_1$  to  $X_1$  will now depend on  $S_2$ .



Finally, we look at the last step in the motif, the conversion of the dynamic response of the adaptive motif  $W$  into  $X_1$ . The instantaneous concentration  $X_1$  should inform the system upon the state of input  $S_1$ . Simple time-integration of  $W$ , similar to the response  $X_2$  (Eq. 4), is not sufficient. While time-integration by itself is important to average over multiple oscillation cycles, it is not sufficient because time-integration with a linear-transfer function does not lead to a change in the response when the amplitude of the input is varied, assuming that the oscillations are symmetric. Indeed to respond to different amplitudes, a non-linear transfer function is required

$$\frac{dX_1}{dt} = k_{X_1} \frac{W^n}{W^n + K_{X_1}^n} - m_{X_1} X_1. \quad (13)$$

These Hill-type non-linear transfer functions are very common in biological systems, for example in gene regulation by transcription factors, or protein activation by multiple enzymes.

## B. Multiplexing

Now that we have specified the model with its components, we characterize its multiplexing capacity, using the formalism of information theory [38]. We define two measures: 1)  $I_1(X_1; A_1)$ , the mutual information between the concentration  $X_1$  and the amplitude  $A_1$  of signal  $S_1$ , and 2)  $I_2(X_2; \mu_2)$ , the mutual information between the concentration  $X_2$  and the concentration level  $\mu_2$  of  $S_2$ . The information capacity of the system is then defined by the total information  $I_T = I_1(X_1; A_1) + I_2(X_2; \mu_2)$  that is transmitted through the system. The mutual information in bits shows how many different input states can be transmitted with 100% fidelity. It does not necessarily reflect whether all input signals are transmitted reliably. For example, increasing the number of input states  $N_A$  can increase the mutual information  $I_1(A_1; X_1)$  [38], yet a specific output concentration  $X_1$  could be less informative about a specific input amplitude  $A_1$ . To quantify the fidelity of signal transmission, we normalize the mutual information by the information entropy  $H(A_1)$  and  $H(\mu_2)$  of the respective inputs. We therefore define the relative mutual information

$$I_R((A_1; X_1), (\mu_2; X_2)) = \frac{I_1(X_1; A_1)}{H(A_1)} + \frac{I_2(X_2; \mu_2)}{H(\mu_2)} \quad (14)$$

$$= \frac{I_1(X_1; A_1)}{\log_2[N_A]} + \frac{I_2(X_2; \mu_2)}{\log_2[N_\mu]}. \quad (15)$$

Note that  $I_R((A_1; X_1), (\mu_2; X_2))$  has a maximum value of 2, meaning that each channel  $i = 1, 2$  transmits all its messages  $S_i \rightarrow X_i$  with 100% fidelity.

The mutual information depends on the kinetic parameters of the system, on the input distribution of the signal

states, and on the amount of noise in the system. In a previous study we have shown that under biologically relevant conditions, a simple biochemical system using only constant signals is capable of simultaneously transmitting at least two bits of information [6], meaning that at least two signals with two input states can be transmitted with 100% fidelity. Here we wondered whether this information capacity can be increased. Therefore, we study the system for increasing number of input states (increasing  $N_A$  for  $S_1$  and  $N_\mu$  for  $S_2$ ), where we assume a uniform distribution of the states for  $S_1$ ,  $A_1 \in [0 : 1]$ , and for  $S_2$ ,  $\mu_2 \in [0 : \mu_{\max}]$  (see Eq. 1). To obtain a lower bound on the information that can be transmitted, we optimize the total mutual information over a subset of the kinetic parameters, where we constrain the kinetic rates between  $10^{-3} < k_i < 10^3$ , the dissociation constants between  $1 < K_i < 7.5 \times 10^4$ , the maximum concentration level for  $S_2$   $10 < \mu_{\max} < 1000$  and the oscillation period  $10 < T < 10000$ . We set the response times of  $X_1, X_2$  to be much longer than the oscillation period, so that the variability in  $V$  and  $W$  due to the oscillations in  $S_1$  is time-integrated; specifically,  $m_{X_1} = m_{X_2} = (NT_p)^{-1} \text{s}^{-1}$ , such that the output averages over  $N = 10$  oscillations with period  $T_p$ . The noise strength is calculated using the linear-noise approximation [39] while assuming that the input signals are constant, of magnitude  $\mu_1, \mu_2$ . The effects of the non-linear and oscillatory nature of the network on the noise strength are thus not taken into account. However, we do not expect that these two effects qualitatively change the observations discussed below. To compute the noise strength, we assume that the maximum copy numbers of  $X_1$  and  $X_2$  are 1000. The optimization is performed using an evolutionary algorithm (see *SI*).

Before we discuss the information transmission capacity of our system, we first show typical results for the time traces and input-output relations as obtained by the evolutionary algorithm. Fig. 3a shows that the oscillations in  $V^P$  are amplified by the adaptive network to yield large amplitude oscillations in  $W^P$ . In contrast,  $X_1$  and  $X_2$  only exhibit very weak oscillations due to their long lifetime. Fig. 3b shows that when  $A_1$  is increased while  $\mu_2$  is kept constant, the average of  $V^P$ , which is set by  $\mu_2$ , is indeed constant. As a result,  $\langle X_2 \rangle$  is constant, as it should be (because  $\mu_2$  is constant). In contrast,  $X_1$  increases with  $A_1$ . This is because the amplitude of the oscillations in  $W^P$  increases with  $A_1$ , which is picked up by the non-linear transfer function from  $W^P$  to  $X_1$ . In addition,  $X_1$  increases because the mean of  $W^P$  itself increases, due to the non-linearity of the network; this further helps to increase  $X_1$  with  $A_1$ . Fig. 3c shows that when  $\mu_2$  is increased while  $A_1$  is kept constant,  $\langle V^P \rangle$  and hence  $X_2$ —the response of  $S_2$ —increases. Importantly, while the mean of the buffer node  $R$  of the adaptive network increases with  $\langle V^P \rangle$ , the mean of the output of this network,  $W^P$ , is almost constant. Consequently,  $X_1$  is nearly constant, as it should because  $X_1$  should reflect the value of  $A_1$  which is kept constant. These two panels

thus show that this system can multiplex two signals: it can transmit multiple states of two signals through one and the same signaling pathway, and yet each output responds very specifically to changes in its corresponding input. This is the central result of our manuscript.

Interestingly, Fig. 3c shows a (very) weak dependence of  $X_1$  on  $S_2 = \mu_2$ , which will introduce crosstalk in the system. It is important to realize that this will reduce information transmission, even in a deterministic noiseless system. The mechanism by which crosstalk can reduce information transmission is illustrated in Fig. 4. Maximal information transmission between  $S_1$  and  $X_1$  occurs if a given amplitude  $A_1$  (independent of  $\mu_2$ ) uniquely maps to a specific output  $X_1$ , and similarly for  $S_2$  and  $X_2$ . In a deterministic system, every combination of inputs ( $S_1, S_2$ ) maps onto a unique combination of outputs ( $X_1, X_2$ ). We aim to multiplex the signals such that  $X_1$  should be a function of  $S_1$  (i.e.  $A_1$ ) only, while  $X_2$  should be a function of  $S_2$  ( $\mu_2$ ) only. That is, the mapping from  $S_i$  to  $X_i$  should be independent of the state of the other signal  $S_{j \neq i}$ . However, crosstalk causes the mapping from  $S_i$  to  $X_i$  to depend on the state of the other channel. This dependence reduces information transmission, because a given concentration of  $X_1$  can now correspond to multiple values of  $A_1$ , as illustrated in Fig. 4a. Crosstalk can thus reduce information transmission even in a deterministic system without biochemical noise.

It is of interest to quantify the amount of information that can be transmitted in the presence of crosstalk in a deterministic, noiseless system. Via the procedure described in the *SI*, we compute the maximal mutual information for the two channels, assuming that we have a uniform distribution of input states for each channel, with  $A_1 \in [0 : 1]$  and  $\mu_2 \in [0 : \mu_{\max}]$ . We find that for channel 2, the mutual information is given by the entropy of the input distribution, which means that the number of signals that can be transmitted with 100% fidelity through that channel is just the total number of input signals for that channel. This is because signal transmission through channel 2 is hardly affected by crosstalk from the other channel. Below we will see and explain that this observation also holds in the presence of biochemical noise. For signal transmission through channel 1, however, the situation is markedly different. The maximum amount of information that can be transmitted through that channel is limited to about 4 bits. This means that up to  $2^4$  signals can be transmitted with 100% fidelity; in this regime, the input signal  $S_1$  can be uniquely inferred from the output signal  $X_1$ . Increasing the number of input signals beyond  $2^4$ , however, does not increase the amount of information that is transmitted through that channel; more signals will be transmitted, but, due to the crosstalk from the other channel, each signal will be transmitted less reliably (see Fig. 4 and *SI*).

We will now quantify how many messages can be transmitted reliably in the presence of not only crosstalk, but also biochemical noise. The results of the optimization of the mutual information using the evolutionary algorithm

are shown in Fig. 5. The left panel shows the relative mutual information for channel 1, the middle panel for channel 2, and the right panel shows the total relative mutual information (Eq. 14). Clearly, biochemical noise affects information transmission through the two respective channels differently.

Firstly, we see that the fidelity of signal transmission through channel 2 is effectively independent of the number of states  $N_A$  that are transmitted through channel 1, even in the presence of biochemical noise (Fig. 5b). This means that channel 2 is essentially insensitive to crosstalk from channel 1. This is because  $X_2$  time-integrates the sinusoidal  $V_P(t)$  via a linear transfer function—the output  $X_2$  is thus sensitive to the mean of  $V_P$  (set by  $S_2$ ), but not to the amplitude of  $V_P(t)$  (set by  $S_1$ ). We also observe that even in the presence of noise, the relative information stays close to 100% when  $N_\mu$  is below 3 bits. Channel 2 is thus fairly resilient to biochemical noise, which can be understood by noting that a linear transfer function (from  $V_p$  to  $X_2$ ) allows for an optimal separation of the  $N_\mu$  input states in phase space [40–42].

The left channel,  $S_1 \rightarrow X_1$ , is more susceptible to noise (Fig. 5a) and to crosstalk from the other channel,  $S_2$ . The susceptibility to noise can be seen for  $N_\mu = 1 \text{ bit} = 2 \text{ states}$ : the relative information decreases as  $N_A$  increases. This sensitivity to noise becomes more pronounced as  $N_\mu$  increases, an effect that is due to the crosstalk from the other channel. A larger  $N_\mu$  reduces the accessible phase space for channel 1—it reduces the volume of state space that allows for a unique mapping from  $S_1$  to  $X_1$ . As a result, a small noise source is more likely to cause a reduction in  $I_R(S_1; X_1)$ . How crosstalk and noise together reduce information transmission is further elucidated in Fig. 4c. Remarkably, even in the presence of noise, maximal relative information is obtained for  $N_A = N_\mu = 4 (= 2 \text{ bits})$  (Fig. 5c), showing that 4 input states can be transmitted for each channel simultaneously without loss of information.

### C. Experimental observations

Here we connect our work to two biological systems. The first system is the p53 DNA damage response system. The p53 protein is a cellular signal for DNA-damage. Different forms of DNA damage exist and they lead to different temporal profiles of the p53 concentration. Double-stranded breaks cause oscillations in the p53 concentration, while single stranded damage leads to a sustained p53 response [5, 43, 44]. Compared to our simple multiplexing motif, the encoding scheme in this system is more involved. In our system two external signals activate the shared component V. In the p53 system, p53 itself is V, but interestingly, negative (indirect) autoregulation of p53 is required to obtain sustained oscillations.

Although the encoding structure is different, the main result is that the system is able to encode two differ-

ent signals into different temporal profiles simultaneously; depending on the type of damage either a constant and/or an oscillatory profile of p53 is present. These two signals could therefore be transmitted simultaneously due to their difference in the temporal profiles. For the p53 system the input signals are binary, e.g. either there is DNA damage or not, although some experiments suggest that the amount of damage also could be transmitted [45]. The maximum information that can be transmitted following our simplified model is much larger than that required for two binary signals. A mathematical model, based upon experimental observations, shows that the encoding step creates a temporal profile for p53 that could be decoded by our suggested decoding module (not shown).

Another system of interest is the MAPK (or RAF-MEK-ERK) signaling cascade. The final output of this cascade is the protein ERK, which shuttles between the cytoplasm and the nucleus. ERK is regulated by many different incoming signals of which EGF, NGF and HRG are well known [46]. The temporal profile of ERK depends on the specific input that is present. NGF and HRG lead to a sustained ERK level [4], while EGF leads to a transient or even oscillatory profile of the ERK level [4, 17, 47]. In comparison with our model ERK would be the shared component V. Experiments show that oscillations in the ERK concentration can arise due to intrinsic dynamics of the system [17]. However, these oscillations could be amplified by, or even arise because of, oscillations in the signal EGF, especially since, to our knowledge, it is unclear what the temporal behavior of EGF is under physiological conditions.

For both experimental systems, we have only described the encoding step. In both cases, two signals are encoded in a shared component V, where one signal leads to a constant response, while the other signal creates oscillations. Both p53 and ERK are transcription factors for many downstream genes [48, 49]. For the decoding of the constant signal, only a simple birth-death process driven by V would be required. Many genes are regulated in this way [25]. The decoding of the oscillatory signal requires an adaptive motif. Although adaptive motifs are common in biological processes [25], it is unclear whether downstream of either p53 or ERK an adaptive motif is present, which would complete our suggested multiplexing motif. As such, our study should be regarded as a proof-of-principle demonstration that biochemical networks can multiplex oscillatory signals.

### III. DISCUSSION

We have presented a scheme for multiplexing two biochemical signals. The premise of the proposal is that the two signals have to be transmitted, not integrated. Indeed, the central hypothesis is that  $X_1$  should only respond to  $S_1$  and  $X_2$  only to  $S_2$ . Information transmission is then maximized when the crosstalk between the

different channels is minimized.

The model discussed here consists of elementary motifs, and can simultaneously transmit two signals reliably. One of these signals is constant in time, and its corresponding information is encoded in its concentration level, while the other signal is dynamic, and its information is encoded in the dynamical properties, but not in its average concentration level. The decoding of the constant signals is performed by a time-integration motif, while the decoding of the oscillatory signal requires a frequency-sensitive motif, for example an adaptive motif.

The main problem in multiplexing biochemical signals is crosstalk between the two signals. In this system the signals are encoded based upon their dynamical profile— $S_1$  is oscillatory and  $S_2$  is constant in time. The decoding module for the oscillatory signal, an adaptive motif, is non-linear. Therefore, this motif is sensitive not only to the temporal properties like the amplitude, but also to the mean or average of its input. This inevitably leads to crosstalk between channel 1 and channel 2, reducing information transmission.

Remarkably, the system is capable of transmitting over 3 bits of information through each channel with 100% fidelity. In the presence of noise the information transmission decreases, but even with considerable noise levels in the biologically relevant regime, more than 2 bits of information can be transmitted through each channel simultaneously; this information transmission capacity is comparable to what has been measured recently in the context of NF- $\kappa$ B signaling [20]. To transmit signals without errors it is preferable to send most information using channel 2 and a smaller number of states through channel 1. The reason for this is twofold. First, channel 2 is less noisy since the number of components is smaller; secondly, channel 1 is corrupted by crosstalk from channel 2, leading to overlaps in the state space of  $X_1$  as a function of  $A_1$  (see Fig. 4). Nonetheless, the two channels can reliably transmit 4 states in the presence of noise. This is a considerable increase in the information transmission compared to a system where both signals are constant in time [6]—this could transmit two binary signals with absolute fidelity. This indicates that oscillatory signals could significantly enhance the information transmission capacity of biochemical systems. Importantly, while we have optimized the parameters of our model system using an evolutionary algorithm, it is conceivable that other architectures than those studied here allow for larger information transmission. Indeed, the results presented here provide a lower bound on information transmission.

In this system we have assumed that the amplitude of the oscillatory signal is the information carrier of that signal. The same analysis could be performed for an oscillatory signal at constant amplitude but with different frequencies. Qualitatively, the results will be similar. The dependence of the gain on the frequency means that the amplitude of the output varies with the frequency of the input (see Fig. 2). The amplitude of the output thus characterizes the signal frequency. However, an intrinsic

sic redundancy is present in using the frequency as the information carrier, which can be understood from the symmetry of the gain (see Fig. 2). The response of the system is equal for frequencies that are positioned symmetrically with respect to the resonance frequency. As a result, for any given output, there are always two possible input frequencies, and without additional information, the cell can not resolve which of the two frequencies is present. Of course, one way to avoid this, would be to use only a part of the gain, in which the gain increases monotonically with frequency.

In this study we have assumed that the input signals are deterministic. Results are obtained following deterministic simulations, where noise is added following a solution of the linear-noise approximation assuming non-oscillatory inputs. The effect of noise is a reduction of the information transmission. However, the effect of noise can always be counteracted by increasing the copy number. At the cost of producing and maintaining more proteins, similar results can therefore be obtained [6]. The effect of oscillations on the variability of the output is small since the response times of  $X_1$  and  $X_2$  are much longer than the oscillation period. Slower responding outputs would time-average the oscillation cycles even more, reducing the variability in the response further.

Transmitting information via oscillatory signals has many advantages. Oscillatory signals minimize the prolonged exposure to high levels of the signal, which can be toxic for cells, as has been argued for calcium oscillations [50]. In systems with cooperativity [51], an oscillating signal effectively reduces the signal threshold for response activation. Pulsed signals also provide a way of controlling the relative expression of different genes [52]. Encoding of stimuli into oscillatory signals can reduce the impact of noise in the input signal and during signal propagation [53]. Frequency encoded signals can be decoded more reliably than constant signals [34].

Here we show that information can be encoded in the amplitude or frequency of oscillatory signals, which are then decoded using a non-linear integration motif. We also discussed two biological systems that may have implemented this multiplexing strategy. The idea to use the temporal kinetics as the information carrier in a signal has been studied in a slightly different context, where the dose information is encoded in the duration of an intermediate component, which in turn is time-integrated by a downstream component [54]. Here, we show that encoding signals into the temporal dynamics of a signaling pathway allows for multiplexing, making it possible to simultaneously transmit multiple input signals through a common network with high fidelity. It is intriguing that systems with a bow-tie structure, such as calcium and NF- $\kappa$ B [20], tend to transmit information via oscillatory signals.

#### IV. MATERIALS AND METHODS

The model is based on mean-field chemical rate equations or the linear-noise approximation [55]. For details see the Supporting Information.

#### ACKNOWLEDGMENTS

We thank José Alvarado for a critical reading of the manuscript.



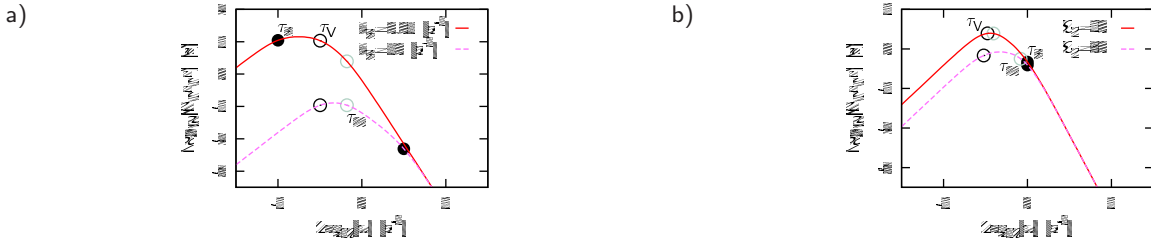


FIG. 2. The gain  $g_{WP}^2(\omega)$  for channel 1 for different parameter sets. The circles indicate the response times  $\tau_i$ . **a)** The effect of changing the timescale  $k_R = \mu_R$ . **b)** The effect of changing the signal  $S_2$  in the other channel 2; it is seen that the gain  $g_{WP}^2(\omega)$  of channel 1 depends on  $S_2$ , which may lead to crosstalk. Parameters: Panel **a)**:  $\mu_2 = 500$ ,  $k_R = m_R$ . Panel **b)**:  $\mu_2 = 200$  and  $\mu_2 = 800$ ,  $k_R = 1$ ,  $m_R = 1$ . Panels **a,b)**:  $\mu_1 = 0$ ,  $k_V = 0.1$ ,  $K_V = 10^{-4}V_T$ ,  $m_V E_T = 600$ ,  $M_V = 5V_T$ ,  $V_T = 1000$ ,  $k_W = 1$ ,  $K_W = M_W = W_T/4$ ,  $W_T = 1000$ ,  $m_W$  sets the timescale.

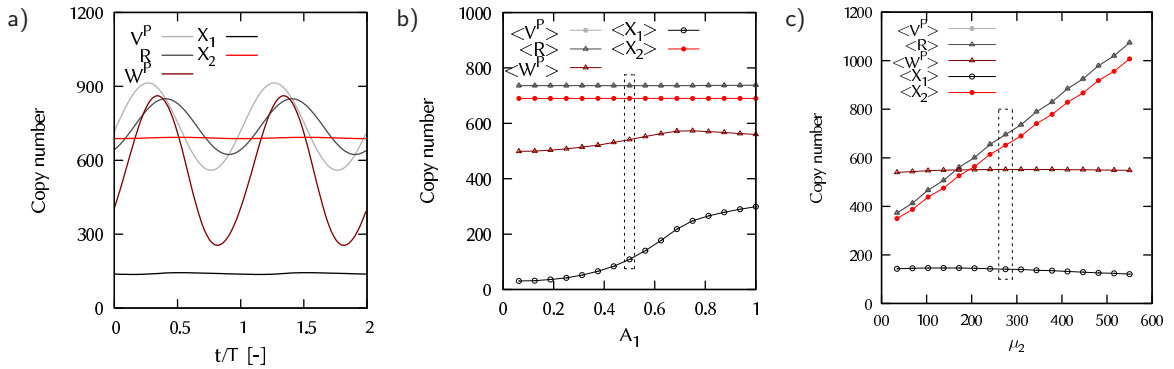


FIG. 3. Typical time traces and input-output curves as obtained by the evolutionary algorithm. Shown are results for a system with  $N_A = N_\mu = 16$ . **a)** Time traces of  $V^P$ ,  $R$ ,  $W^P$ ,  $X_1$  and  $X_2$  for  $A_1 = 0.5$  and  $\mu_2 = 275$  **b)**  $\langle V^P \rangle$ ,  $\langle R \rangle$ ,  $\langle W^P \rangle$ ,  $\langle X_1 \rangle$ , and  $\langle X_2 \rangle$  as a function of  $A_1$ , keeping  $\mu_2 = 275$  constant. **c)**  $\langle V^P \rangle$ ,  $\langle R \rangle$ ,  $\langle W^P \rangle$ ,  $\langle X_1 \rangle$ , and  $\langle X_2 \rangle$  as a function of  $\mu_2$ , keeping  $A_1 = 0.5$ . The figure shows that the system can multiplex:  $X_1$  is sensitive to  $S_1 = A_1$  (panel b) but not  $S_2 = \mu_2$  (panel c), while  $X_2$  is sensitive to  $S_2 = \mu_2$  (panel c) but not  $S_1 = A_1$  (panel b). The time traces in panel a correspond to the points in panels b and c that are indicated by the dashed lines. All panels correspond to the point in Fig. 5c.

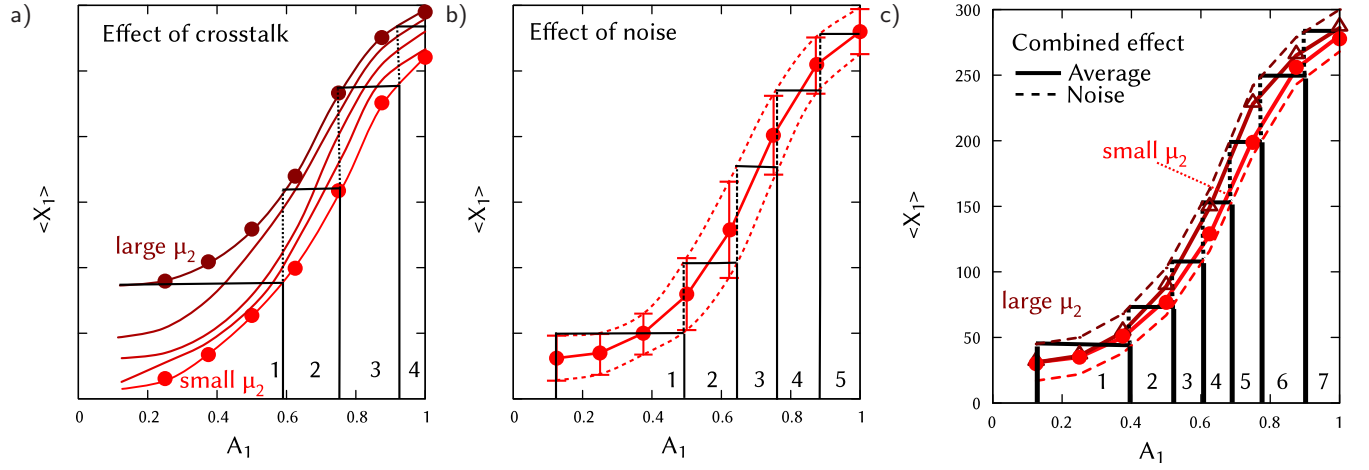


FIG. 4. The influence of noise and crosstalk on information transmission in pathway  $S_1 \rightarrow X_1$ . **a)** Schematic: Crosstalk reduces the amount of information that can be transmitted. For every  $A_1$  multiple values of  $\langle X_1 \rangle$  are obtained, each corresponding to a different value of  $\mu_2$ . The dark red corresponds to the maximum value of  $\langle X_1 \rangle$  for each  $A_1$ , while the light red line denotes the minimum value. The black line in between the red lines visualizes the range for which a specific  $\langle X_1 \rangle$  uniquely maps to a single input amplitude  $A_1$ . Crosstalk from the  $S_2 \rightarrow X_2$  channel thus limits the number of states, and hence the amount of information, that can be transmitted through channel 1. **b)** Schematic: Also noise reduces the number of input states that can be resolved. Shown is the mean response curve  $\langle X_1 \rangle(A_1)$  together with the noise in  $X_1$ . Dotted lines give the minimum and maximum values of  $X_1$  for each amplitude. Since for each  $A_1$  a larger range of  $X_1$  values is obtained, less states  $A_1$  can be uniquely encoded in the phase space. This is reflected in the width of the boxes; indeed, here only 5 input states can be transmitted with absolute reliability. **c)** Combined effect of noise and crosstalk on information transmission for a system with  $N_A = N_\mu = 8$ , as obtained from the evolutionary optimization algorithm; the results corresponds to the black dot in Fig. 5c. Both the noise and the crosstalk reduce the number of possible input states that can be transmitted. Solid lines give the deterministic dose-response curve, while dashed lines correspond to a network with noise. Dark red lines indicate the maximum of  $\langle X_1 \rangle$  for a specific  $A_1$  over the range of possible values of  $\mu_2$ , while red lines give the minimum value. Because for each  $A_1$  a range of  $\langle X_1 \rangle$  values is obtained, the number of states  $A_1$  that can be uniquely encoded in the phase space is limited. This is reflected in the increase in the width of the boxes; indeed, here only 7 input states can be transmitted with absolute reliability.

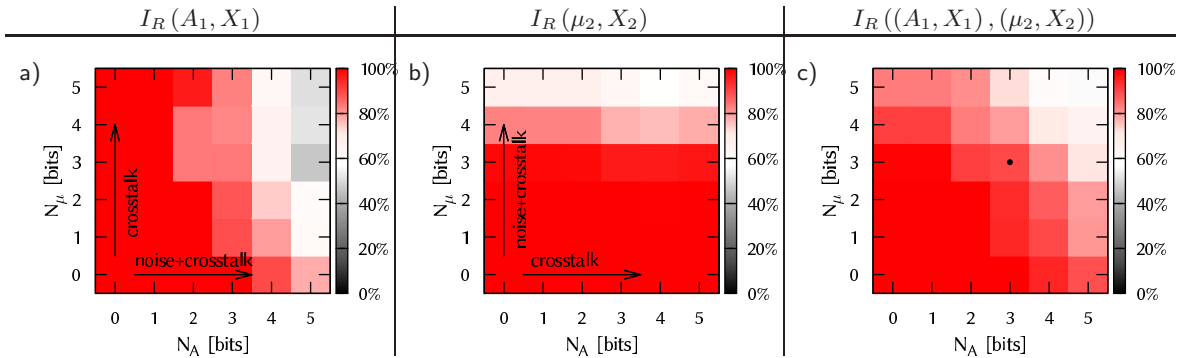


FIG. 5. The transmitted relative information  $I_R$  (Eq. 14) as function of the number of input states  $N_A, N_\mu$ , where 2 bits correspond to  $2^2 = 4$  input states. Results are shown for a stochastic system with  $X_T = 1000$ . In panels **a,b** 100% corresponds to  $I_R = 1$ , while in **c** 100% corresponds to  $I_R = 2$ . **a)** the relative mutual information  $I_R(A_1, X_1)$  for the  $S_1 \rightarrow X_1$  channel; the total mutual information is obtained by multiplying  $I_R$  with  $\log_2(N_A)$ , the horizontal axis. Both the decrease in  $I_R(A_1, X_1)$  as a function of  $N_A$  due to the presence of biochemical noise and the decrease in  $I_R(A_1, X_1)$  as a function of  $N_\mu$  due to the presence of crosstalk is observed. **b)** the relative mutual information  $I_R(\mu_2, X_2)$  for the  $S_2 \rightarrow X_2$  channel. The total mutual information is obtained by multiplying  $I_R$  with  $\log_2(N_\mu)$ , the vertical axis. The effect of noise is relatively small and crosstalk from  $S_1$  is hardly present. **c)** the relative information of the total network  $I_R((A_1, X_1), (\mu_2, X_2)) = I_R(A_1, X_1) + I_R(\mu_2, X_2)$ . The dot corresponds to the timetraces in Fig. 3. All results are obtained through numerical optimization (see SI).

## Supplementary information: Multiplexing oscillatory biochemical signals

Wiet de Ronde and Pieter Rein ten Wolde

### V. GENERAL DEFINITIONS

We use the following two general definitions for the mean and the maximum of a specific component, if the period of the input signal is  $T_p$

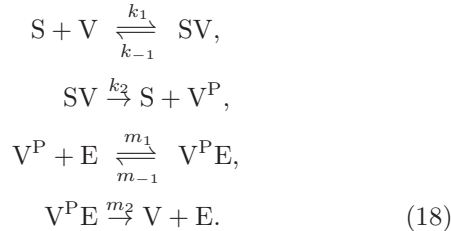
$$\langle Z \rangle = \frac{1}{T_p} \int_t^{t+T_p} Z(t') dt', \quad (16)$$

$$Z_{\max} = \sup_{T_p} Z(t). \quad (17)$$

#### A. Encoding

##### 1. MM-approximation

In the derivation of Eq. 3 of the main text, we have assumed, as is commonly done, Michaelis-Menten (MM) kinetics. However, the MM-approximation may not hold for a dynamical system [56, 57], since the MM-approach is a coarse graining of the full mass-action kinetics of the system. Therefore we numerically evaluate whether the MM-approximation is valid for our network. The full set of reactions is (see Eq. 2 of the main text)



The quasi-steady-state approximation in MM-kinetics assumes that the concentration of the complex of enzyme and substrate is in equilibrium and does not change (or changes very slowly) with time, leading to

$$\frac{dSV}{dt} = 0, \quad \frac{dV^P E}{dt} = 0. \quad (19)$$

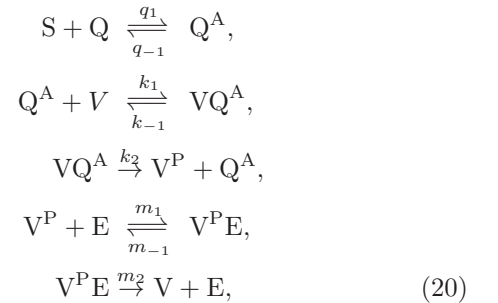
We compare the results for the full system (described by Eq. 18), with the Michaelis-Menten approximation in the linear regime (Eq. 2 of the main text), in which the phosphorylation reaction is linear in the signal concentration  $S$  (Fig. 6a). Eq. 2 of the main text is obtained for  $K_V (= (k_{-1} + k_2)/k_1) \ll V_T - V^P$ , such that the phosphorylation reaction of  $V$  to  $V^P$  simplifies to  $k_V \sum_i S_i(t)$  (Eq. 3 of the main text), which is indeed linear in  $S_i$  and zero-order in  $V$ . If  $V_T \gg S$ , the linearity condition will also be fulfilled for all moments in time when the system

is dynamical [56]. In this case all  $S$  directly binds to  $V$  and the complex  $SV$  is very stable.

This very stable complex  $SV$ , however, is likely to influence the dynamics of the signal oscillations, as in the following two examples: if the oscillations in the signal  $S$  are driven due to factors external of the cell (like hormone pulsing), or if the oscillations depend on the (saturated) degradation of the signal  $S$  [58] and this regulation does not act on the signal in bound form. Due to the stability of the complex, in the rising part of the oscillation  $S$  directly forms the complex  $SV$ , but, again because of the stability, during the falling part of the oscillation  $SV$  does not dissociate. Since the complex is not regulated, the total signal level  $S_T = S + SV$  increases, since with every oscillation the concentration  $SV$  increases, until all  $V$  is saturated. As a result, the oscillatory dynamics of the signal is strongly influenced: the periodicity is reduced and the mean level of signal present is increased (Fig. 6b).

The interaction between the signal  $S$  and  $V$  may corrupt the information that is encoded in the oscillations (Fig. 6b), because it influences the oscillation characteristics. To overcome this, instead of assuming  $S \ll V$ , one could assume  $V \ll S$ . However, in this regime it is unclear whether the dynamical behavior of the MM-approximation accurately represents the dynamics of the full mass-action equations. Moreover, if  $S \gg V$ , a small minimum concentration  $S_{\min}$  directly saturates all the  $V$  molecules. As a result, the concentration of  $V$  is insensitive to any oscillation in the concentration  $S$  when the minimum concentration  $S_{\min}$  is larger than the concentration  $V$ .

Therefore, an extended model is required, with two additional reactions Eq. 20. This extension is biologically inspired, since many external signals are sensed by receptors  $Q$ , which in turn activate (or phosphorylate) intracellular proteins. The crucial ingredient is that the signal-bound receptor dissociates on a much faster timescale than the oscillations. Due to this very fast receptor dissociation, the signal-bound state is very small.



With this biological-inspired, small extension, the dose-response curve is similar to the dose-response curve for the Michaelis-Menten approximation with small  $K_V$  (in the linear regime), also for oscillatory signals (Fig. 6c).

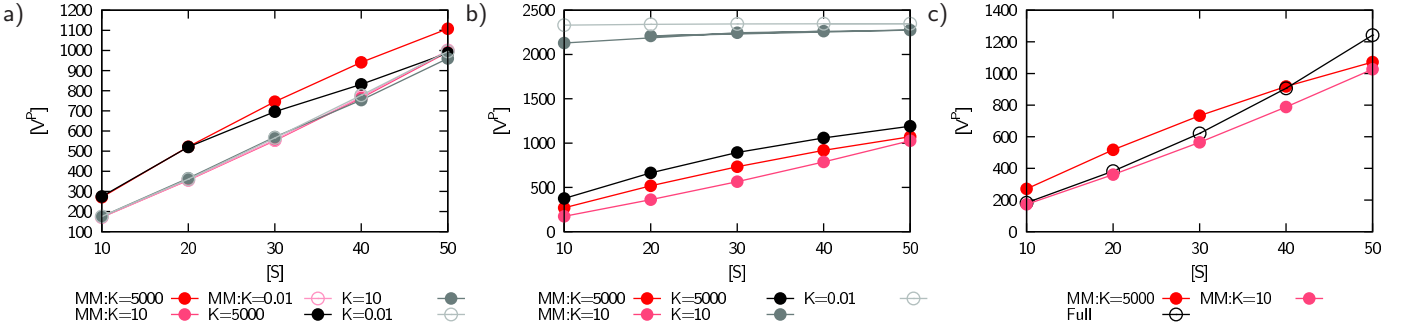


FIG. 6. Comparison of the results of the Michaelis-Menten approximation (red) with those of the full mass action equation (Eq. 18, black) using Gillespie simulations. **a)** Dose-response curve for *constant* signal  $S$ . The Michaelis-Menten approximation describes the full system (Eq. 18) very well (only for  $K = 5000$  the curves do not precisely overlap). **b)** Dose-response for *sinusoidal* input  $S$  with  $T = 100$  s. Due to the strong complex formation of  $VS$  all the signaling molecules  $S$  bind  $V$  until all  $V$  is saturated and, as a result, the signal does not oscillate independently of the system. Accordingly, the effective concentration  $S$  is much larger than the mean of the oscillations. Parameters:  $r_1 s_{-1}, E_T = 150, V_T = 2500, M_V = 5000$ , and for  $K_V = 5000, K_V = 10, K_V = 0.01$  respectively  $\{k_{-1}, k_2, m_{-1}, m_2\} = \{4997.5, 2.5, 4999, 1\} s^{-1}, \{9, 1, 4998, 2\} s^{-1}, \{0, 1, 4998, 2\} s^{-1}$ , and  $k_1(S) = 10, 10, 1000 s^{-1}$  respectively **c)** The dose-response curve of the extended model described by Eq. 20 compared to the Michaelis-Menten equations of Eq. 3 of the main text. It is seen that the MM model of Eq. 3 of the main text accurately describes the dynamics of the extended system of Eq. Eq. 20. Parameters:  $q_1(S) = 2.5 s^{-1}, q_{-1} = 4000 s^{-1}, k_1 V_T = 5000 s^{-1}, k_{-1} = 4000, k_2 = 25 s^{-1}, m_1 E_T = 100 s^{-1}, m_{-1} = 4998 s^{-1}, m_2 = 1 s^{-1}, E_T = 50, R_T = 1000, V_T = 5000$ .

## B. Linear Approximation

In this section we show that the MM-approximation in the linear regime (see Eq. 3 of the main text) does not change the mean of  $V^P$ ,  $\langle V^P \rangle$ , irrespective of the signal characteristics. We compare analytical results with numerical simulations and for completeness we compare this linear regime (I) with two other regimes which we describe in more detail below: zero-order dynamics for  $V$  (II) and non-linear phosphorylation (III).

In regime II there are many more  $V_T$  molecules than kinase ( $S_i$ ) and phosphatase ( $E_T$ ) molecules. Therefore, the kinase and phosphatase enzymes are *both* saturated ( $V_T \rightarrow \infty$ ). Since saturation of both kinase and phosphatase molecules implies that  $M_V, K_V \ll V_T$ , the dynamics of Eq. 2 of the main text can be simplified to

$$\frac{dV^P}{dt} \approx k_V \left( \sum_i S_i(t) \right) - m_V. \quad (21)$$

This is the well-known regime of zero-order dynamics for  $V$ . In this regime ( $V^P$ ) can be approximated by a binary function  $\langle V^P \rangle = 0$  or  $\langle V^P \rangle = V_T$ , where the transition occurs at a critical kinase concentration  $(\sum_i S_i)_{\text{crit}}$  (see Fig. 7, open black symbols).  $V$  thus acts as a switch. A switch-like functional dependence of  $V$  on  $S$  does not lead to perfect tracking of the signal  $S$ , and therefore not to accurate propagation of the oscillations.

The third regime, regime III, is in a sense the opposite of the previous. In this regime,  $V$  is limiting (e.g.  $M_V, K_V \gg V_T$ , see Eq. 2 of the main text). Eq. 2 of the

main text then reduces to

$$\frac{dV^P}{dt} = k'_V \left( \sum_i S_i(t) \right) (V_T - V^P) - m'_V V^P, \quad (22)$$

where  $k'_V = k_V/K_V$  and  $m'_V = m_V E_T/M_V$ . In this regime, the phosphorylation and dephosphorylation reaction are first order in  $V$  and  $V^P$ , respectively. A typical dose-response curve is shown in Fig. 7 (closed gray symbols).

In regime I, corresponding to Eq. 3 of the main text, the two preceding regimes are combined (Fig. 7, closed red symbols). There is saturation of the kinases in the production, but saturation of  $V^P$  in the dephosphorylation, leading to

$$\frac{dV^P}{dt} = k_V \left( \sum_i S_i(t) \right) - m'_V V^P, \quad (23)$$

which is Eq. 3 of the main text.

In Fig. 7a the dose-response curve for  $V^P$  as function of  $S$  is shown; the focus is on the mean  $\langle V^P \rangle$  as a function of a constant signal  $S$  with increasing mean  $\mu$ . Regime I of the main text (closed red symbols) has an approximate linear relation between  $S$  and  $\langle V^P \rangle$ . Regime II (open black symbols) shows the switch-like response, while regime III (closed gray symbols) increases hyperbolically to saturation.

A sinusoidal oscillation can only be propagated perfectly as a sinusoidal signal if the dose-response function is linear. For non-linear dose-response functions, oscillations with small amplitude are propagated correctly, since for small perturbations every function has linear characteristics. However, larger amplitude oscillations



are deformed by the non-linear transfer function. As a result, the mean  $\langle V^P \rangle$  changes as a function of  $A$  and/or  $T$ , the oscillation parameters. A stronger non-linear dose-response function decreases the amplitude-range of oscillations that can be propagated without this deformation. Figure 7b shows  $\langle V^P \rangle$  for signals with different properties  $A$  and  $T$ , but constant signal mean  $\mu$ . If the transfer function allows for perfect tracking of the input signal,  $\langle V^P \rangle$  should be constant because the mean  $\mu$  is constant. Indeed, in both regime I and III  $\langle V^P \rangle$  does not depend on the oscillation parameters  $A, T$ , while in regime II a strong dependence on these parameters exist.

For completeness, in Fig. 8a-c we show corresponding time traces. Again the strong non-linear response for regime II (Fig. 8b) is observed, while regime I (Fig. 8a) and III (Fig. 8c) exhibit oscillations that are very similar to the sinusoidal oscillations of the input signal. Please also note the reduction in amplitude in regime III (Fig. 8c), compared to regime I of the main text (Fig. 8a). This can be explained by the hyperbolic shape of the dose-response curve for regime III, which dampens changes in  $S$  (Fig. 7a).

## C. Numerical optimization: a two-step rocket

### 1. General characteristics

The numerical optimization used to produce Fig. 5 of the main text is based on the Wright-Fisher model for population evolution. In each simulation a population of  $N$  independent systems is initialized. Each system consists of a single multiplexing network. In the initialization step, each network is assigned random parameters where each parameter is within the ranges specified in Eq. 25 and Eq. 26. In the next step the fitness of each network is calculated, which we detail in the following subsection. Based on the fitness  $I_T$  for each network, in the selection step again  $N$  new systems are chosen from the original  $N$  systems. The likelihood of selection (reproduction) of each system is proportional to its fitness  $I_T$ . Each new network is then ‘‘mutated’’ by multiplying all kinetic parameters by the factor  $(1 + \delta)$ , where  $\delta$  is drawn uniform randomly from the range  $[\Delta: \Delta]$ ; we take  $\Delta = 0.3$ . Then the cycle is repeated.

#### a. Parameters

We take the kinetic parameters of the encoding module to be fixed, to ensure correct propagation of the oscillations to component  $V$ . For a reliable transmission of oscillations, the phosphorylation of  $V$  is given by Eq. 3 of the main text, as discussed in the previous section. We further take the mean of the oscillatory signal to be

constant, resulting in the following fixed parameters

$$\begin{aligned} k_V &= 1/10 \text{ s}^{-1}, \\ m_V E_T &= 5625 \text{ s}^{-1}, \\ M_V/V_T &= 30, \\ K_V/V_T &= 1/250, \\ V_T &= 2500, \\ \mu_1 &= 25 \end{aligned} \tag{24}$$

Next, the following parameters are constrained based upon values of other parameters

$$\begin{aligned} k_W &\text{ to set } \langle W^P \rangle = W_T/2 \text{ for a constant signal,} \\ m_{X_2} &= m_{X_1} = (10T)^{-1}, \\ k_{X_2} &= 5m_{X_2}, \\ k_{X_1} &= X_T m_{X_1} \left( \frac{W_T^{n_{X_1}}}{W_T^{n_{X_1}} + K_{X_1}^{n_{X_1}}} \right)^{-1} \end{aligned} \tag{25}$$

The parameters  $X_T = W_T = 1000$  are constant (unless explicitly mentioned).

This leads to the following set of parameters that are optimized for given  $N_A, N_\mu$ , where between square brackets we give the minimum and maximum value of each parameter.

$$\begin{aligned} K_W &[1 : 75000], \\ M_W &[1 : 75000], \\ m_W &[10^{-3} \text{ s}^{-1} : 10^3 \text{ s}^{-1}], \\ T &[10^1 \text{ s} : 10^4 \text{ s}], \\ \mu_{2,\max} &[10 : 1000], \\ n_{X_1} &[1 : 5], \\ K_{X_1} &[1 : 75000]. \end{aligned} \tag{26}$$

### 2. Step 1: Contiguity

A key point is that, while the precise mapping from  $S$  to  $X$  may not be critical for the total amount of information transmitted *per se*, this is likely to be important for whether or not this information can be exploited [6]. We therefore impose the multiplexing requirement [6] (see Fig. 9).

To illustrate the multiplexing requirement, imagine that each signal  $S_i$  can take 3 levels:  $S_i^0, S_i^1, S_i^2$  (Fig. 9). This means that both  $X_1$  and  $X_2$  each have 9 states, corresponding to the  $3 \times 3$  possible combinations of input states; for each state of the input signal  $S_i$ , *i.e.*  $S_i^k$ , we thus have 3 output states of  $X_i$ , corresponding to the three different states of the other input signal. The multiplexing requirement now imposes that the mapping from  $S_1, S_2$  to  $X_1, X_2$  is such that the output states  $\{X_i\}$  corresponding to input  $S_i = j$  are grouped into sets that are contiguous and increase monotonically with  $j$ , for

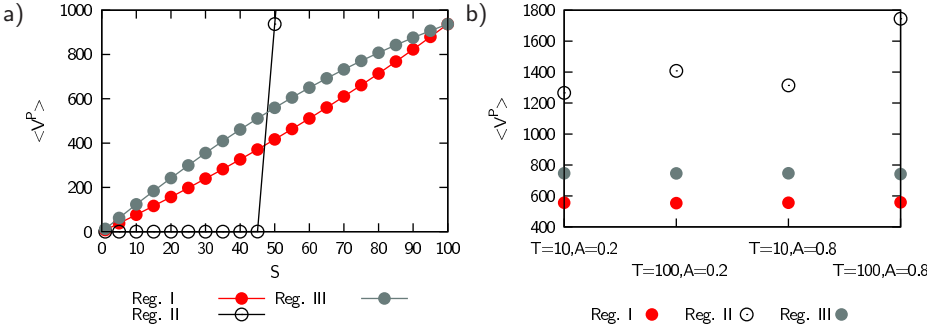


FIG. 7. **a)** The dose-response curve is shown for the regime in which both the production and degradation are zero-order in  $V^P$  (regime II, Eq. 21), in which both production and degradation are first order in  $V^P$  (regime III, Eq. 23), and, the model of the main text, zero-order production but linear degradation of  $V^P$  (regime I, Eq. 22). The curve that is linear over the widest  $S$ -range is that for linear degradation of  $V^P$ , but zero-order production, studied in the main text (regime I). Parameters: Regime I:  $m_V E_T = 500$ ,  $K_V/V_T = 1/25000$ ,  $M_V/V_T = 2$ ;  $k_V = 1 \text{ s}^{-1}$ ; Regime II:  $m_V E_T = 50$ ,  $K_V/V_T = 1/25000$ ,  $M_V/V_T = 1/25000$ ; Regime III:  $m_V E_T = 100$ ,  $K_V/V_T = 2$ ,  $M_V/V_T = 2$ ; **b)** The time average over a single oscillation period,  $\langle V^P \rangle_T$ , is shown for four different simulations where the signal characteristics are as indicated and  $\mu_S = 50$ .

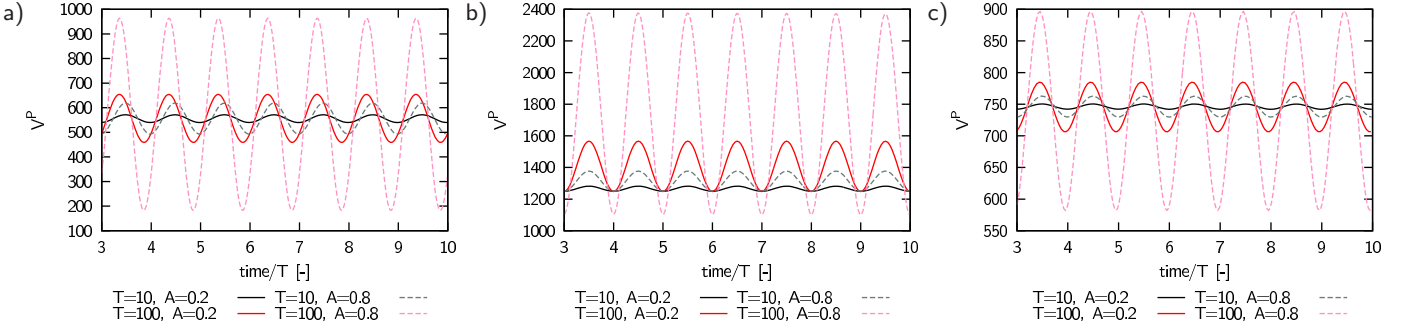


FIG. 8. Time traces for regime I (panel a), with first-order degradation of  $V^P$  and zero-order production of  $V$  (Eq. 3 of the main text); regime II (panel b), with zero-order production and degradation of  $V$  (Eq. 21); regime III (panel c), with first-order production and degradation of  $V$  (Eq. 22). In all cases, the amplitude  $A$  and frequency  $T^{-1}$  are varied, while keeping  $\mu = 50$ . The non-linear response for the zero-order dynamics in regime II is clearly visible in b. The difference between panel a and c is the amplitude of the response. The system of the main text with linear production of  $V^P$  (I, panel a) has a much larger amplitude than that with saturated production of  $V^P$  (III, panel c); note the different scale of the y-axis.

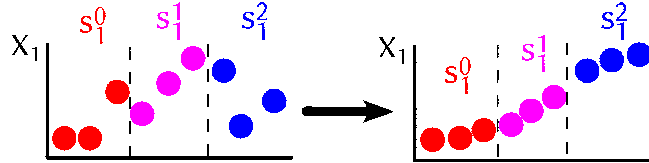


FIG. 9. Schematic view of the contiguity requirement. For a system with 3 states of  $S_1, S_2$ , the corresponding output states of  $X_1$  should follow a contiguous (and thus monotonic) order. In other words, the three states of  $X_i$  that correspond to one given state of  $S_i$  are grouped into a set; the different sets  $\{X_i\}$  that correspond to the different states of the input  $S_i$  increase monotonically with  $S_i$ .

each signal  $i$ . In other words, the three states of  $X_i$  that correspond to one given state of  $S_i$  are grouped into a set; the different sets  $\{X_i\}$  that correspond to the different states of the input  $S_i$  increase monotonically with  $S_i$ . This leads to a monotonic input-output relation between  $S_i$  and  $X_i$  for each  $i$ , which can be decoded by the

network.

Mutual information does not enforce contiguity. Optimizing mutual information only means minimizing the overlap of the conditional probability distributions  $p(X_i|S_i^k)$  corresponding to the different states  $k$  of the input  $S_i$ . Certainly in the absence of noise, where each

combination of inputs  $S_1, S_2$  yields one and only one combination of outputs  $X_1, X_2$ , a minimal overlap of the conditional distribution does not impose a contiguous division; in essence, the outputs  $X_1$  and  $X_2$  are  $\delta$ -peaks, which could in principle be arranged in any order when the networks are optimized for maximizing the mutual information. This, we argue, hampers decoding. Therefore, the first step in the optimization routine is to enforce a contiguous mapping.

For a *deterministic network* we obtain a contiguous split by the following procedure: At each step of the evolutionary algorithm we determine for all input states  $(S_1^k, S_2^{k'}) = (A_1^k, \mu_2^{k'})$ , the output concentrations  $\langle X_1 \rangle^{k,k'}, \langle X_2 \rangle^{k,k'}$ . For a specific state  $k$  of the input signal  $S_1^k, A_1^k$ , we determine the minimum and maximum value of  $\langle X_1 \rangle^{k,k'}$ , which (most likely) correspond to  $\langle X_1 \rangle$  for  $\mu_{2,\min}$  and  $\mu_{2,\max}$  respectively. We thus obtain for each state  $k$  of  $S_1$  a set or “block” of  $\langle X_1 \rangle$  values between  $\{\langle X_{1,\min} \rangle, \langle X_{1,\max} \rangle\}$  (see also Fig. 4 of the main text). Similar blocks are obtained for  $\langle X_2 \rangle$  for each state  $k'$  of  $S_2$ , where the block boundaries depend on  $S_1$ , *i.e.*  $A_{1,\min}, A_{1,\max}$ .

The fitness of each network is then determined by the amount of overlap between the different blocks corresponding to the different states of signal  $S_i$ , where an increase in overlap reduces the fitness. An overlap means that from an output level  $X_i$  the state of the input  $S_i$  cannot uniquely be inferred. Maximum fitness therefore corresponds to minimal overlap between the blocks.

For a *stochastic network* the optimization method is slightly different. Instead of determining the boundaries of the block by the minimum and maximum output concentration, we now include the noise. Using the linear-noise approximation, we determine for each output concentration  $\langle X_i \rangle$  the corresponding variance  $\sigma_{X_i}^2$ . The block is then formed by  $\{[\langle X_i \rangle - \sigma_{X_i}]_{\min}, [\langle X_i \rangle + \sigma_{X_i}]_{\max}\}$ , where  $\sigma_{X_i}$  is the noise determined through the linear-noise approximation as described in the main text. The evolutionary algorithm optimizes each network using a minimum overlap as selection criterion, similar to the deterministic network.

### 3. Step 2: Mutual information

The procedure outlined above generates networks with optimal contiguity [6]. To quantify information transmission in these networks we compute the mutual information. Specifically, the performance measure is the multiplication of the relative mutual information of the individual channels

$$I_T = \frac{I(S_1, X_1)}{H(S_1)} \times \frac{I(S_2, X_2)}{H(S_2)}, \quad (27)$$

where  $H(S_1)$  is the entropy of the amplitude input distribution  $p(A_1)$ ;  $H(S_2)$  is the entropy of the concentration

input distribution  $p(\mu_2)$ ; and  $I(S_i, X_i)$  is the mutual information between  $S_i$  and  $X_i$  [38].

To determine the entropy of the input distribution and the mutual information we need to specify the form of the input distributions. We take the input distributions to be uniform:

$$p(A_1 = a) = \frac{1}{N_A}, \text{ with amplitude values} \\ a_i = \frac{i}{N_A}, i \in [1 : N_A], \quad (28)$$

$$p(\mu_2 = \mu) = \frac{1}{N_\mu} \text{ with concentration values} \\ \mu_j = \frac{j}{N_\mu} \mu_{\max}, j \in [1 : N_\mu], \quad (29)$$

where  $\mu_{\max}$  is an optimization parameter with maximum value 1000.

To compute the mutual information, we have used a slightly different approach for the stochastic and the deterministic networks.

#### a. Mutual information for a stochastic network

To calculate the mutual information  $I(S_i; X_i)$  for a stochastic network, we determine for all input states  $(S_1^k, S_2^{k'}) = (A_1^k, \mu_2^{k'})$ , the output concentrations  $\langle X_1 \rangle, \langle X_2 \rangle$  and corresponding variances  $\sigma_{X_1}^2, \sigma_{X_2}^2$  via the linear-noise approximation. With these quantities the mutual information of the two respective channels are calculated via

$$I(S_i, X_i) = H(X_i) - H(X_i|S_i), \quad (30)$$

where  $H(X_i) = -\sum_l p(X_i^l) \ln p(X_i^l)$  and  $H(X_i|S_i) = -\sum_k p(S_i^k) \sum_l p(X_i^l|S_i^k) \ln p(X_i^l|S_i^k)$ . Here,  $p(X_i^l|S_i^k) = \sum_{k'} p(S_j^{k'} \neq i) p(X_i^l|S_i^k, S_j^{k'} \neq i)$ , where  $p(X_i^l|S_i^k, S_j^{k'} \neq i)$  is a Gaussian distribution centered around the mean  $\langle X_i \rangle$  given by  $S_i^k$  and  $S_j^{k'}$ .

#### b. Mutual information for a deterministic network

For a deterministic network without noise in the mean field limit, each input  $(S_i^k, S_j^{k'})$  maps onto a unique output  $(X_i^{k,k'}, X_j^{k,k'})$  which is a delta peak. One may therefore think that when the number of input states for each signal goes to infinity, the mutual information also goes to infinity; this would imply that an infinite number of states for each signal  $S_i$  could be transmitted with 100% fidelity. However, this is not true: the mutual information and hence the number of signals that can be transmitted with 100% fidelity, remains bounded because of the crosstalk (and the finite copy number). As described in the text, crosstalk means that the input-output mapping no longer is unique; from the output  $X_i$ , the input  $S_i$  can no longer be inferred with 100% fidelity.

To compute the maximum amount of information that can be transmitted through each channel, we adopt the following procedure. We first take the number of states  $N_i$  that is transmitted through each channel  $i$  to be finite. We thus discretize each signal  $S_i$  with equally spaced values  $S_i^k$ , with  $k = 0, \dots, N_i$ . Signal  $S_1$  is discretized between  $[A_{\min} - 1]$  and signal  $S_2$  between  $[\mu_{\min} - \mu_{\max}]$ ;

only  $A_{\min}$  and  $\mu_{\min}$  depend on the number of states; the maximum values are constant. For each  $S_i^k$ , we compute  $X_i^{k,k'}$  for each state of the other input signal  $S_j^{k'}_{j \neq i}$  by solving the mean-field network in steady state. We then determine the minimum and maximum values of  $X_i^{k,k'}$  for a given  $k$ ,  $X_{i,\min}^k$  and  $X_{i,\max}^k$ . This is equivalent to the ‘‘block’’-procedure, described above. Next, we calculate  $H(X_i^k|S_i^k) = -\int_{X_{i,\min}^k}^{X_{i,\max}^k} dX_i^k p(X_i^k|S_i^k) \ln p(X_i^k|S_i^k)$ ,

with  $p(X_i^k|S_i^k) = 1/(X_{i,\max}^k - X_{i,\min}^k)$  for each state  $k$  of signal  $S_i$ ,  $S_i^k$ . To compute  $H(X_i|S_i)$ , we now have to average  $H(X_i^k|S_i^k)$  over all  $S_i^k$ :  $H(X_i|S_i) = -\sum_k p(S_i^k)H(X_i^k|S_i^k)$ . The entropy of the output distribution is  $H(X_i) = -\sum_l p(X_i^l) \ln p(X_i^l)$ , where  $p(X_i) = \sum_k p(S_i^k)p(X_i^k|S_i^k)$ .

Fig. 10a shows the mutual information  $I(S_1; X_1)$  as function of the of the number of states  $N_A$  in channel 1, for  $N_\mu = 16$  states of channel 2. It is seen that initially the mutual information increases linearly with  $N_A$ ; moreover, the slope is unity. In this regime, the number of states that can be transmitted with 100% fidelity through channel 1 is the total number of states of that channel. In essence, the different blocks of states  $X_1$  corresponding to the different states of  $S_1$  do not overlap, which means that from the output  $X_1$ , the input  $S_1$  can be uniquely inferred. However, as  $N_A$  increases beyond 4 bits, the different blocks overlap increasingly, and the number of signals that can be transmitted with 100% fidelity saturates; in the plateau regime, increasing the number of input signals further no longer increases the number of signals that can be transmitted reliably. The plateau value slightly depends on the number of signals  $N_\mu$  that are transmitted through channel 2, which is shown in panel b. It is seen that the plateau value saturates to about 3.74 bits when  $N_\mu$  is larger than 3.5 bits. We thus conclude that the maximum number of signals that can be transmitted with 100% fidelity through channel 1 is about 4 bits.

Fig. 10c shows the mutual information  $I(S_2, X_2)$  as a function of  $N_\mu$ , for  $N_A = 16$ . Clearly, the mutual information is to an excellent approximation given by the entropy of the input distribution over the full range of  $N_\mu$ , which means that all signals can be transmitted with 100% fidelity, even when the number of signals goes beyond 4 bits. This is because the effect of crosstalk from the other channel is negligible, as explained in the main text.



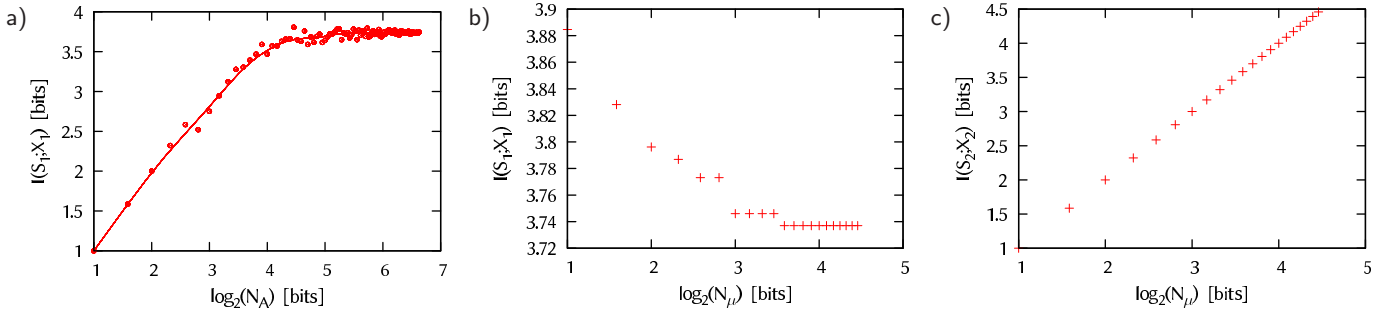


FIG. 10. The effect of crosstalk on information transmission in a deterministic system. **a)** The mutual information  $I(S_1; X_1)$  as function of the number of states  $N_A$ , with  $N_\mu = 16$ . The line is to guide the eye. **b)** The plateau value of  $I(S_1; X_1)$  as a function of  $N_A$  for a given  $N_\mu$  (see panel a), plotted against  $N_\mu$ . It is seen that beyond  $N_\mu = 3.5$ , the plateau value is constant. **c)** The mutual information  $I(S_2; X_2)$  as a function of  $N_\mu$  for  $N_A = 16$ . It is seen that the mutual information is equal to the entropy of the input distribution. This is because the effect of crosstalk is negligible. The results are obtained for a network that has been optimized via the procedure described in section VC 2 with  $N_A = N_\mu = 16$ , and with  $A_1$  in the range  $[0 - 1]$  and  $\mu_2$  in the range  $[0 - 23]$ ; the optimized value of  $\mu_2^{\max} = 23$  as found by the procedure described in VC 2 is lower than the maximally allowed value  $\mu_2^{\max} = 1000$ , because that mimizes the effect of crosstalk from channel 2 on channel 1. Parameters:  $m_w = 0.006\text{s}^{-1}$ ,  $K_W/W_T = 1.6 \times 10^{-2}$ ,  $M_W/W_T = 7.9 \times 10^{-2}$ ,  $K_{X_1}/X_T = 1 \times 10^2$ ,  $n_{X_1} = 3$ ,  $X_T = W_T = 100$ .

- 
- [1] Schwartz MA, Madhani HD (2004) Principles of MAP kinase signaling specificity in *Saccharomyces cerevisiae*. *Annual Review of Genetics* 38: 725–48.
- [2] Rensing L, Ruoff P (2009) How can yeast cells decide between three activated MAP kinase pathways? A model approach. *Journal of Theoretical Biology* 257: 578–587.
- [3] Marshall CJ (1995) Specificity of receptor tyrosine kinase signaling: transient versus sustained extracellular signal-regulated kinase activation. *Cell* 80: 179–85.
- [4] Sasagawa S, Ozaki Yi, Fujita K, Kuroda S (2005) Prediction and validation of the distinct dynamics of transient and sustained ERK activation. *Nature cell biology* 7: 365–73.
- [5] Batchelor E, Loewer A, Mock C, Lahav G (2011) Stimulus-dependent dynamics of p53 in single cells. *Molecular Systems Biology* 7: 1–8.
- [6] de Ronde W, Tostevin F, Ten Wolde PR (2011) Multiplexing Biochemical Signals. *Physical Review Letters* 107: 1–4.
- [7] Patterson JC, Klimenko ES, Thorner J (2010) Single-cell analysis reveals that insulation maintains signaling specificity between two yeast MAPK pathways with common components. *Science signaling* 3: 1–11.
- [8] Behar M, Dohlman HG, Elston TC (2007) Kinetic insulation as an effective mechanism for achieving pathway specificity in intracellular signaling networks. *Proceedings of the National Academy of Sciences of the USA* 104: 16146–51.
- [9] Bardwell L, Zou X, Nie Q, Komarova NL (2007) Mathematical models of specificity in cell signaling. *Biophysical journal* 92: 3425–41.
- [10] McClean MN, Mody A, Broach JR, Ramanathan S (2007) Cross-talk and decision making in MAP kinase pathways. *Nature genetics* 39: 409–14.
- [11] Hu B, Rappel WJ, Levine H (2009) Mechanisms and constraints on yeast MAPK signaling specificity. *Biophysical journal* 96: 4755–63.
- [12] Thalhauser CJ, Komarova NL (2009) Specificity and robustness of the mammalian MAPK-IEG network. *Biophysical journal* 96: 3471–82.
- [13] Hu B, Levine H, Rappel Wj (2011) Design principles and specificity in biological networks with cross activation. *Physical biology* 8: 026001.
- [14] Berridge MJ, Lipp P, Bootman MD (2000) The versatility and universality of calcium signalling. *Nature reviews Molecular cell biology* 1: 11–21.
- [15] Hoffmann A, Levchenko A, Scott ML, Baltimore D (2002) The I $\kappa$ B-NF- $\kappa$ B signaling module: temporal control and selective gene activation. *Science* 298: 1241–5.
- [16] Nelson DE, Ihekweaba AEC, Elliott M, Johnson JR, Gibney CA, et al. (2004) Oscillations in NF- $\kappa$ B signaling control the dynamics of gene expression. *Science (New York, NY)* 306: 704–8.
- [17] Shankaran H, Ippolito DL, Chrisler WB, Resat H, Bollinger N, et al. (2009) Rapid and sustained nuclear-cytoplasmic ERK oscillations induced by epidermal growth factor. *Molecular systems biology* 5: 332.
- [18] Ashall L, Horton CA, Nelson DE, Paszek P, Harper CV, et al. (2009) Timing and Specificity of NF- $\kappa$ B Dependent Transcription. *Science* 324: 242–246.
- [19] Sung MH, Salvatore L, De Lorenzi R, Indrawan A, Pasparakis M, et al. (2009) Sustained oscillations of NF- $\kappa$ B produce distinct genome scanning and gene expression profiles. *PloS one* 4: e7163.
- [20] Cheong R, Rhee A, Wang CJ, Nemenman I, Levchenko A (2011) Information transduction capacity of noisy biochemical signaling networks. *Science* 334: 354–358.
- [21] Wu Z, Chui C, Hong G, Chang S (2011) Physiological analysis on oscillatory behavior of glucose insulin regulation by model with delays. *Journal of Theoretical Biology* : 1–9.
- [22] Li Y, Goldbeter A (1989) Frequency specificity in intercellular communication. Influence of patterns of periodic signaling on target cell responsiveness. *Biophysical journal* 55: 125–45.
- [23] Behar M, Hoffmann A (2010) Understanding the temporal codes of intra-cellular signals. *Current Opinion in genetics & development* 20: 684–93.
- [24] Goldbeter A, Koshland DE (1981) An amplified sensitivity arising from covalent modification in biological systems. *Proceedings of the National Academy of Sciences of the United States of America* 78: 6840–4.
- [25] Alon U (2007) *An Introduction to Systems Biology: Design Principles of Biological Circuits*. *Mathematical and Computational Biology Series*, Vol. 10. Chapman and Hall/CRC.
- [26] Detwiler PB, Ramanathan S, Sengupta A, Shraiman BI (2000) Engineering aspects of enzymatic signal transduction: Photoreceptors in the retina. *Biophysical journal* 79.
- [27] Ziv E, Nemenman I, Wiggins CH (2007) Optimal signal processing in small stochastic biochemical networks. *PloS one* 2: e1077.
- [28] Tkačik G, Callan C, Bialek W (2008) Information capacity of genetic regulatory elements. *Physical Review E* 78: 1–17.
- [29] Walczak AM, Mugler A, Wiggins CH (2009) A stochastic spectral analysis of transcriptional regulatory cascades. *Proceedings of the National Academy of Sciences of the USA* 106: 6529–34.
- [30] Mehta P, Goyal S, Long T, Bassler BL, Wingreen NS (2009) Information processing and signal integration in bacterial quorum sensing. *Molecular systems biology* 5: 325.
- [31] Tostevin F, Ten Wolde PR (2009) Mutual Information between Input and Output Trajectories of Biochemical Networks. *Physical Review Letters* 102: 1–4.
- [32] Tsai TYC, Choi YS, Ma W, Pomerening JR, Tang C, et al. (2008) Robust, tunable biological oscillations from interlinked positive and negative feedback loops. *Science (New York, NY)* 321: 126–9.
- [33] Stricker J, Cookson S, Bennett MR, Mather WH, Tsimring LS, et al. (2008) A fast, robust and tunable synthetic gene oscillator. *Nature* 456: 516–9.
- [34] Tostevin F, de Ronde W, Ten Wolde PR (2012) Reliability of frequency and amplitude decoding in gene regulation. In preparation .
- [35] de Ronde W, Tostevin F, Ten Wolde PR (2010) Effect of feedback on the fidelity of information transmission of time-varying signals. *Physical Review E* 82.
- [36] Tostevin F, Ten Wolde PR (2010) Mutual information

- in time-varying biochemical systems. *Physical Review E* 81: 061917.
- [37] Ma W, Trusina A, El-Samad H, Lim WA, Tang C (2009) Defining network topologies that can achieve biochemical adaptation. *Cell* 138: 760–73.
- [38] Shannon CE (1948) The mathematical theory of communication. *The Bell System Technical Journal* 27: 379–423,623–656.
- [39] van Kampen NG (2007) *Stochastic Processes in Physics and Chemistry*. North-Holland: Elsevier, third edition.
- [40] Tkačik G, Walczak AM, Bialek W (2009) Optimizing information flow in small genetic networks. *Physical Review E* 80: 1–18.
- [41] Tkačik G, Walczak AM (2011) Information transmission in genetic regulatory networks: a review. *Journal of Physics: Condensed matter* 23: 153102.
- [42] Tkačik G, Walczak AM, Bialek W (2012) Optimizing information flow in small genetic networks. iii. a self-interacting gene. *Phys Rev E* 85: 041903.
- [43] Fei P, El-Deiry WS (2003) p53 and radiation responses. *Oncogene* 22: 5774–83.
- [44] Sengupta S, Harris CC (2005) p53: traffic cop at the crossroads of DNA repair and recombination. *Nature reviews Molecular cell biology* 6: 44–55.
- [45] Lahav G, Rosenfeld N, Sigal A, Geva-Zatorsky N, Levine AJ, et al. (2004) Dynamics of the p53-Mdm2 feedback loop in individual cells. *Nature genetics* 36: 147–50.
- [46] Shaul YD, Seger R (2007) The MEK/ERK cascade: from signaling specificity to diverse functions. *Biochimica et biophysica acta* 1773: 1213–26.
- [47] Kholodenko BN (2000) Negative feedback and ultrasensitivity can bring about oscillations in the mitogen-activated protein kinase cascades. *European journal of biochemistry / FEBS* 267: 1583–8.
- [48] von Kriegsheim A, Baiocchi D, Birtwistle MR, Sump-ton D, Bienvenut W, et al. (2009) Cell fate decisions are specified by the dynamic ERK interactome. *Nature cell biology* 11: 1458–64.
- [49] Wei CL, Wu Q, Vega VB, Chiu KP, Ng P, et al. (2006) A global map of p53 transcription-factor binding sites in the human genome. *Cell* 124: 207–19.
- [50] Trump BF, Berezsky IK (1995) Calcium-mediated cell injury and cell death. *FASEB* 9: 219–228.
- [51] Gall D, Baus E, Dupont G (2000) Activation of the liver glycogen phosphorylase by Ca(2+) oscillations: a theoretical study. *Journal of theoretical biology* 207: 445–54.
- [52] Cai L, Dalal CK, Elowitz MB (2008) Frequency-modulated nuclear localization bursts coordinate gene regulation. *Nature* 455: 485–90.
- [53] Rapp PE, Mees AI, Sparrow CT (1981) Frequency encoded biochemical regulation is more accurate than amplitude dependent control. *Journal of theoretical biology* 90: 531–44.
- [54] Behar M, Hao N, Dohlman HG, Elston TC (2008) Dose-to-duration encoding and signaling beyond saturation in intracellular signaling networks. *PLoS computational biology* 4: e1000197.
- [55] Elf J, Ehrenberg M (2003) Fast evaluation of fluctuations in biochemical networks with the linear noise approximation. *Genome research* 13: 2475–84.
- [56] Segel LA (1988) On the validity of the steady state assumption of enzyme kinetics. *Bulletin of Mathematical Biology* 50: 579–593.
- [57] Tzafiriri A, Edelman ER (2007) Quasi-steady-state kinetics at enzyme and substrate concentrations in excess of the Michaelis-Menten constant. *Journal of theoretical biology* 245: 737–48.
- [58] Mengel B, Hunziker A, Pedersen L, Trusina A, Jensen MH, et al. (2010) Modeling oscillatory control in NF- $\kappa$ B, p53 and Wnt signaling. *Current Opinion in genetics & development* 20: 656–64.